PHYSICS

Magnetic and defect probes of the SmB_6 surface state

Lin Jiao[1]*, Sahana Rößler[1], Deepa Kasinathan[1], Priscila F. S. Rosa[2,3], Chunyu Guo[4,5], Huiqiu Yuan[4,5,6], Chao-Xing Liu[7], Zachary Fisk[2], Frank Steglich[1,4,8], Steffen Wirth[1]*

The impact of nonmagnetic and magnetic impurities on topological insulators is a central focus concerning their fundamental physics and possible spintronics and quantum computing applications. Combining scanning tunneling spectroscopy with transport measurements, we investigate, both locally and globally, the effect of nonmagnetic and magnetic substituents in SmB_6, a predicted topological Kondo insulator. Around the so-introduced substitutents and in accord with theoretical predictions, the surface states are locally suppressed with different length scales depending on the substituent's magnetic properties. For sufficiently high substituent concentrations, these states are globally destroyed. Similarly, using a magnetic tip in tunneling spectroscopy also resulted in largely suppressed surface states. Hence, a destruction of the surface states is always observed close to atoms with substantial magnetic moment. This points to the topological nature of the surface states in SmB_6 and illustrates how magnetic impurities destroy the surface states from microscopic to macroscopic length scales.

INTRODUCTION

Topological surface states (TSSs) are novel quantum electronic states that not only serve as a playground for realizing many exotic physical phenomena (such as magnetic monopoles, Majorana fermions, and the quantum anomalous Hall effect) but also may have several fascinating applications, e.g., in spintronics or quantum computing (*1*). These states are theoretically predicted to be robust against backscattering from nonmagnetic impurities due to their chiral spin texture, whereas a magnetic impurity breaks time-reversal symmetry and therefore induces spin scattering. Within the framework of the Anderson impurity model, however, the spin of a magnetic impurity may also be screened by the conduction electrons via the Kondo effect, resulting in an effectively nonmagnetic scattering center at sufficiently low temperature (*2*).

SmB_6 was theoretically predicted to be a topological Kondo insulator in which a direct bulk gap is induced by Kondo hybridization, and the TSSs reside in this small bulk gap (*3*–*5*). Compared to weakly correlated topological insulators, SmB_6 features a small but fully opened bulk gap (*6*). Therefore, the TSSs dominate the density of states (DOS) at the Fermi level E_F at low temperature, such that insulating bulk and metallic surface properties can be well distinguished in spectroscopic (*7*) and transport measurements (*8*). In addition, the small bulk gap can easily be suppressed by doping, converting the system to a trivial insulator (*9*). Moreover, SmB_6 establishes a Kondo lattice system in which even nonmagnetic impurities may generate magnetic scattering by locally increasing the DOS or by creating a "Kondo hole" in the lattice. All these aspects call for a detailed study of the local sensitivity of the surface states in SmB_6 to nonmagnetic and magnetic impurity atoms or magnetic moments in close proximity to the surface.

Although the metallic nature of the surface states in SmB_6 has been confirmed by several experiments (*8*, *10*, *11*), pinning down their topological origin remains challenging and controversial (*12*–*14*). Consequently, detecting the spin texture of the metallic surface states is cardinal and crucial. Considerable efforts have been made to uncover the helical spin texture of the surface state by spin-resolved angle-resolved photoelectron spectroscopy (*15*, *16*) and spin injection (*17*). However, the surface conditions are multifarious (*18*). Therefore, investigations on well-defined and nonreconstructed surfaces are important, and a microscopic probe is called for. In this respect, scanning tunneling microscopy and spectroscopy (STM/S) studies have demonstrated their ability to characterize the bulk and surface state band of SmB_6 (*19*–*21*). In particular, the dominating peak in the low-temperature ($T \lesssim 7$ K) tunneling spectra at a bias voltage $V_b \approx -6.5$ mV was shown to contain contributions from both the bulk and the surface state (*7*). Here, we track the response of this peak to the close proximity of magnetic moments, either attached to the tunneling tip or within the sample surface, to investigate the fate of the surface states. We further studied the local and global impact of nonmagnetic and magnetic impurities on the surface states by comparing microscopic STS with macroscopic transport measurements.

RESULTS

STS with magnetic tips

To investigate the −6.5-mV signature peak and its link to the surface state in more detail, we compare STS spectra obtained by a regular (nonmagnetic) W tip and a magnetic Cr-coated tip on the same surface of pristine SmB_6. Cr-coated tips are often used for spin-dependent STS [(*22*) and references therein]. Figure 1 shows the tunneling spectra at 0.35 K on a nonreconstructed surface (see Fig. 2A). At large $|V_b| \gtrsim 20$ meV, the spectra measured by the two tips are very similar and featureless, indicating that any difference is not due to an exotic DOS of the tips (*23*). For small $|V_b| \lesssim 20$ meV, however, the two differential conductance (dI/dV) spectra are markedly different: In the case of the Cr tip, the pronounced signature peak at −6.5 meV is markedly suppressed, likely due to a pronounced suppression of tunneling into the surface states. Because this peak contains components from bulk and surface states, such a suppressed tunneling into surface states then exposes the direct bulk hybridization gap, albeit slightly reduced in size (*7*, *19*, *21*). This is corroborated by a notable similarity of spectra obtained with a magnetic Cr tip and such recorded with a W tip at 20 K (text S2 and fig. S4), a temperature at which the surface states do not yet manifest themselves in tunneling spectra (*7*). In addition, as we will show later, scanning with a W tip over the surface of Gd-substituted SmB_6 generates

[1]Max Planck Institute for Chemical Physics of Solids, Nöthnitzer Straße 40, 01187 Dresden, Germany. [2]Department of Physics and Astronomy, University of California, Irvine, CA 92697, USA. [3]Los Alamos National Laboratory, Los Alamos, NM 87545, USA. [4]Center for Correlated Matter, Zhejiang University, Hangzhou 310058, People's Republic of China. [5]Department of Physics, Zhejiang University, Hangzhou 310058, People's Republic of China. [6]Collaborative Innovation Center of Advanced Microstructures, Nanjing University, Nanjing 210093, People's Republic of China. [7]Department of Physics, The Pennsylvania State University, University Park, PA 16802, USA. [8]Institute of Physics, Chinese Academy of Sciences, Beijing 100190, People's Republic of China.
*Corresponding author. Email: LinJiao@cpfs.mpg.de (L.J.); wirth@cpfs.mpg.de (S.W.)

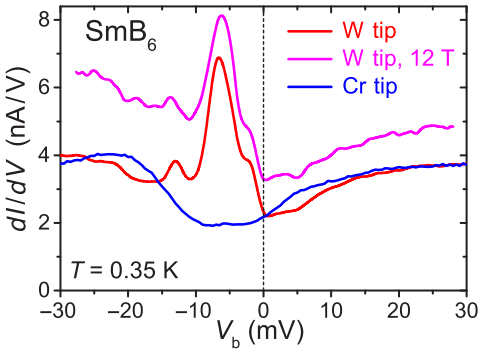

Fig. 1. Tunneling spectra with W and Cr tips. Spectra obtained on nonreconstructed surfaces of pure SmB_6 by a W tip (red) and a magnetic Cr tip (blue) at 0.35 K and zero magnetic field (V_b = 50 mV; set-point current I_{sp} = 200 pA). For comparison, a spectrum taken with a W tip at a magnetic field of 12 T is presented (pink, vertically offset by 1 nA/V).

a similar reduction of the −6.5-meV peak at low temperatures. In this case, the W tip may pick up magnetic Gd substitutents from the surface, and this process can even be reversed (see text S1 and fig. S2). Picking up Gd from the sample converts a regular W tip into a magnetic tip as, e.g., observed by STM on $Fe_{1+y}Te$ where excess Fe atoms were picked up (*24*). The close similarity of the spectra obtained with these two types of magnetic tips suggests that the spectral changes are induced by the magnetic nature of the tips, consistent with a spin texture at the surface of SmB_6 (*25*). However, the reduction in dI/dV upon using magnetic tips, reaching 72% at V_b = −6.5 mV, is, to the best of our knowledge, extraordinarily large and beyond expectations for spin-polarized STS (*22*). Thus, spin-polarized tunneling alone, based on an in-plane alignment of the Dirac electron spins, may not account for this very effective suppression of the signature peak at −6.5 meV. This is even more obvious in view of a spin polarization of less than 50% for a Cr tip (*26*). Moreover, a tunneling spectrum obtained at $\mu_0 H$ = 12 T is rather similar to zero-field spectra for regular W tips (Fig. 1) and precludes the possibility of a magnetic stray field of the magnetic tip suppressing the surface state locally (see also fig. S1).

Surface states around magnetic and nonmagnetic substituents

To scrutinize the effect of magnetism on the surface states of SmB_6, we now investigate the local impact of substituents, both nonmagnetic (Y) and magnetic (Gd), on these surface states. In particular, we focus on the peak at V_b = −6.5 mV as this peak exhibits the strongest response to the development of the surface states at low T (*7*). Therefore, we refer to it as surface state signature peak, despite the fact that bulk states also contribute.

Figure 2 exhibits representative topographies (8 nm by 8 nm field of view) of a pristine sample (Fig. 2A), a 3% Y-substituted sample (SmB_6:3%Y; Fig. 2B), and a 0.5% Gd-substituted sample (SmB_6:0.5% Gd; Fig. 2C) (see also text S3 and figs. S3 and S5). By comparison to earlier work (*18*, *20*, *27*) on pristine SmB_6, we infer that these surfaces are B terminated. The surface of pure SmB_6 is very clean (Fig. 2A), exhibiting only very few defects. The protrusions seen in this topography are likely nonmagnetic (or of only small magnetic moment), as suggested by their negligible spectral response to magnetic fields of up to 12 T (*7*). Comparing the surfaces of the substituted samples to pristine SmB_6 reveals the expected higher density of defects in the former, and one can safely assume that the protrusions in substituted samples predominantly represent the substituents (text S5 and fig. S7), a fact that is also supported by the spectroscopic results below. In addition, the observation of W tips changing into magnetic ones after they picked up atoms (or clusters) from Gd-substituted SmB_6 surfaces suggests the involvement of magnetic constituents, i.e., Gd, in the picked-up entities.

In the following, we obtained STS spectra on nonreconstructed, B-terminated surfaces on which we focused on areas with only very few defects (see also text S4 and fig. S6). Figure 2 (D to F) represents spectra taken along the cyan arrows shown in the respective topographies (Fig. 2, A to C); i.e., spectra #1 were taken on top of the respective defects, whereas spectra of increasing number were obtained for increasing distance from the impurity. The tunneling spectra obtained at T = 0.35 K sufficiently far away from the defects are notably similar for all samples. This finding demonstrates that within the current substitution level, any influence of the defects is highly local in nature, regardless of the magnetic properties of the substituent. However, very close to—and specifically on top of—the substituents, there are marked differences between the pure and Y-substituted SmB_6 on the one hand and the Gd-doped sample on the other hand: For nonmagnetic defects (Fig. 2, D and E), the surface state signature peak is only moderately suppressed, whereas in Gd-substituted SmB_6, all low-energy features appear largely suppressed close to the magnetic substituent, and the spectrum is reminiscent of those observed with Cr tips, indicating a common origin of the peak suppression.

To allow for a quantitative analysis of the impurity effect, we plot the intensities of the dI/dV spectra at −6.5 and −2.5 meV as a function of the distance from the defects in Fig. 2 (G to I). Note that the additional shoulder at about −2.5 meV is exclusively related (*7*) to the surface states [likely to the heavy quasiparticle surface states (*28*)]. Both peaks (dashed lines in Fig. 2, G to I) recover in a similar fashion upon going away from the defects in these samples, but ℓ_{sup} and, specifically, h_{sup} are quite different (h_{sup} and ℓ_{sup} describe the peak intensity suppression at the defect and the extent of this suppression, respectively). Peak intensities have regained their values on unperturbed surfaces at $\ell_{sup} \lesssim 1.5$ nm for pristine and Y-substituted SmB_6 and $\ell_{sup}^{Gd} \approx 2.2$ nm for Gd-substituted SmB_6. The recovery of the surface state with increasing distance from the defect follows the prediction by theoretical models (*29*, *30*) in which the Dirac electrons of the topological surface state are assumed to be locally coupled to a magnetic impurity through exchange coupling. Intuitively, this model describes the suppression of the surface state DOS around the magnetic impurity due to a local gap opening and the distance-dependent behavior of surface state DOS away from the magnetic impurity. The dashed-line fits are described in text S6; h_{sup} and ℓ_{sup} are obtained from the respective curves. On top of the nonmagnetic defects, the TSSs still survive. Although the abovementioned model is not intended to be applied to nonmagnetic impurities, we made use of the fact that it describes the experimental data reasonably well to still obtain h_{sup} and ℓ_{sup}. The apparent applicability of the theoretical model to nonmagnetic impurities along with the moderate suppression ($h_{sup} \approx$ 15 to 45%) may be due to the local changes of the bulk band structure (*29*–*31*) and/or the Kondo hole effect (*32*, *33*). On the other hand, the large magnetic moment of Gd locally breaks time-reversal symmetry and may eventually gap out the Dirac cone states. As a result, h_{sup}^{Gd} reaches 70% at the Gd defect, reminiscent of the value obtained using a Cr tip. We also observed a similar influence of magnetic substituents on the tunneling spectra in weakly correlated topological insulators, such as Cr-substituted (*34*–*36*) or V-substituted (*37*) Sb_2Te_3. Our observation of an only local impact of magnetic substituents on the surface state is consistent with an unexpectedly insensitive response of the TSSs

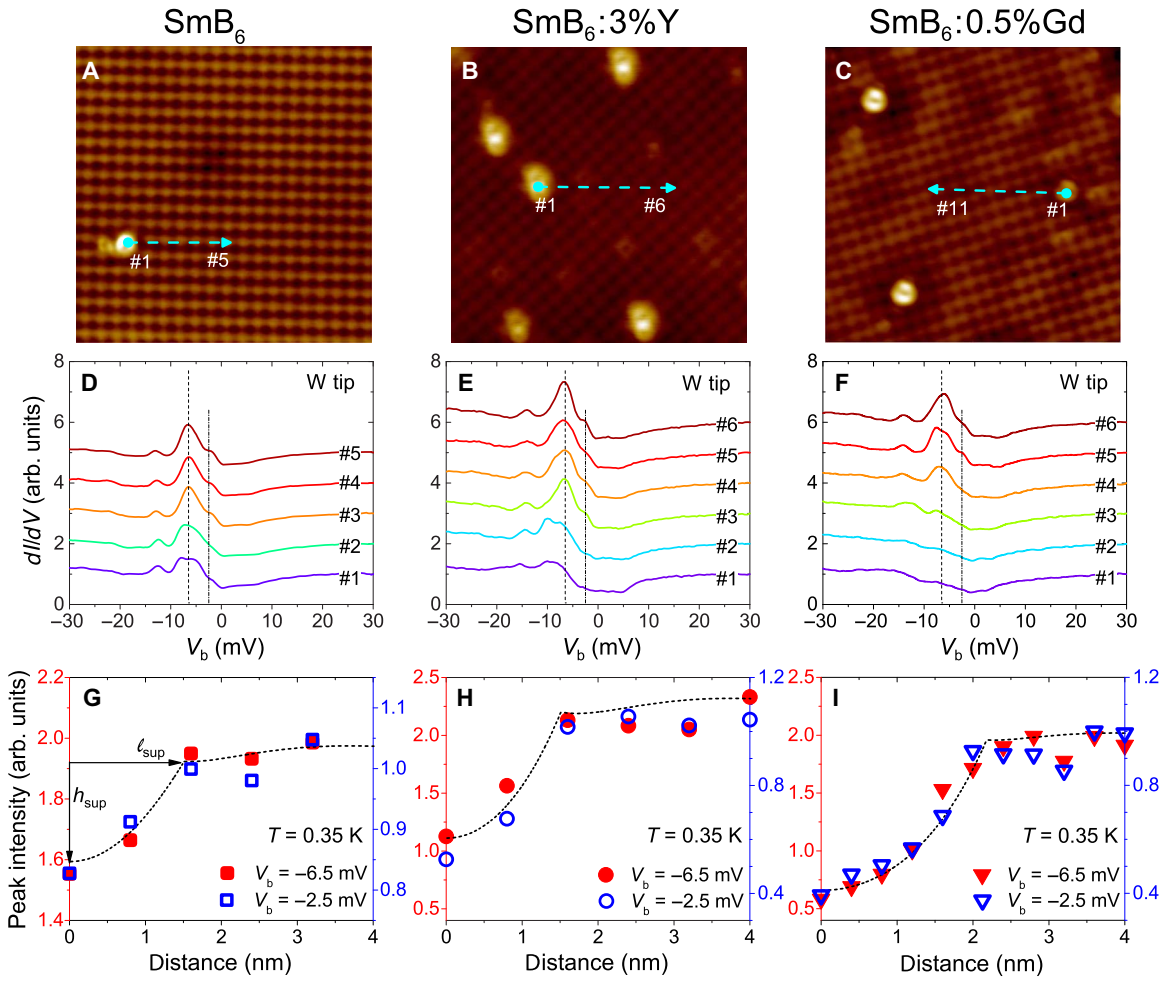

Fig. 2. Influence of impurities on spectroscopic results. (**A** to **C**) Topographies (8 nm by 8 nm) of pure SmB_6 as well as SmB_6:3%Y and SmB_6:0.5%Gd. The cyan arrows indicate the ranges and directions of STS measurements around the impurities. (**D** to **F**) *dI/dV* curves of the three samples measured at 0.35 K and zero field. The curves are measured at positions with increasing distance from the impurity (the impurities are located at #1) along the arrows in (A) to (C), correspondingly (V_b = 30 mV; I_{sp} = 100 pA). arb. units, arbitrary units. (**G** to **I**) *dI/dV* values at V_b = −6.5 meV (red) and −2.5 meV (blue) with increasing distance from the impurity (impurities are located at 0). The black dashed lines are fits according to the model (see text S6). h_{sup} and ℓ_{sup} indicate the suppression of peak intensity at the impurity and its lateral extent, respectively.

in Bi_2Se_3 to magnetic impurities at low impurity concentration in a macroscopic measurement (*38*).

As shown above, the TSSs are fully recovered around 2.2 nm from the Gd substituent site. For SmB_6:0.5%Gd, the average distance between Gd substituents is ~2.4 nm. A pressing question at this juncture is, what if the average Gd-Gd distance is reduced to well below ℓ_{sup}, i.e., if the areas of suppressed surface states sufficiently overlap? To address this, we also probed a SmB_6:3%Gd with an average Gd-Gd distance of about 1.3 nm (text S4 and fig. S6).

From a microscopic to a macroscopic length scale

The resistivity $\rho(T)$ of pure SmB_6 exhibits a well-known saturation below around 3 K, which is due to surface conductance (see Fig. 3A) (*10*, *11*). We find a very similar behavior for SmB_6:3%Y and SmB_6:0.5% Gd samples, yet with a much smaller overall change in $\rho(T)$ due to the substituents. For SmB_6:3%Gd, the low-T saturation of $\rho(T)$ is not observed; instead, $\rho(T)$ continues to increase exponentially, indicating a remaining gap. This is expected when the average Gd-Gd distance is smaller compared to ℓ_{sup}^{Gd}. In highly, nonmagnetic substituted SmB_6 (see example of SmB_6:18%Y in Fig. 3), the $\rho(T)$ behavior is qualitatively different from nonsubstituted or lightly substituted samples, possibly due to interacting substitutents.

The data presented in Fig. 3B allow an estimate of the changes exerted on the bulk hybridization gap Δ from $\rho(T) \propto \exp(\Delta/k_BT)$, where k_B is the Boltzmann constant. Pure SmB_6 exhibits the typical two gap values (*39*) with $\Delta_1 \approx 3.1$ meV for 5 K $\leq T \leq$ 12 K and $\Delta_2 \approx 5.2$ meV for 20 K $\leq T \leq$ 40 K (the latter is marked in Fig. 3B). For the lightly (≤3%) substituted samples, somewhat reduced gap values (*40*) of $\Delta_1 \approx 2.1$ meV (9 K $\leq T \leq$ 14 K) and $\Delta_2 \approx 4.3$ meV at higher T are observed, along with an increased surface conductivity, all in line with a substitution-induced modification of the Kondo lattice formation (*8*). Yet, these changes in the bulk are minute and apparently too small to account for the marked changes in the surface properties. Above ~10 K, the resistivities are determined by the bulk band structure, and the measured values perfectly overlap for the lightly substituted samples. In contrast, $\rho(T)$ of the highly substituted sample SmB_6:18%Y below ~20 K deviates from exponential behavior.

The resistivity data in Fig. 3 provide compelling support from a global measurement for the local picture obtained from STS (Fig. 2): Around a magnetic substituent, the disturbance is stronger and extends

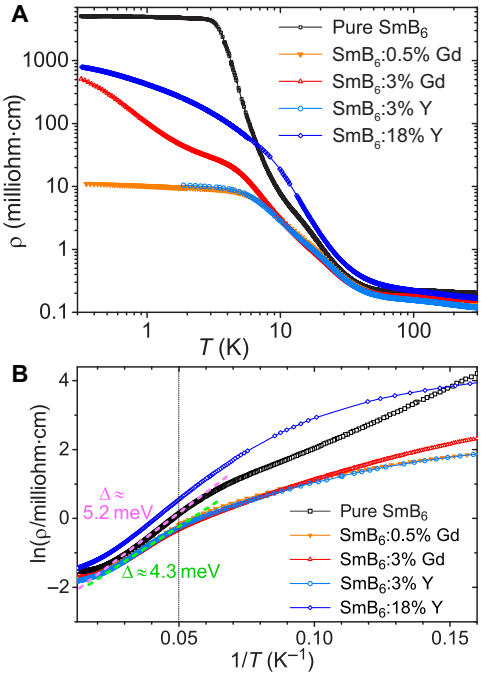

Fig. 3. Resistivity of pristine and substituted SmB_6. (**A**) Temperature dependence of resistivity ρ of pure and differently substituted SmB_6 in double-logarithmic presentation. (**B**) ln(ρ) versus 1/*T* plot at intermediate temperatures used to derive the energy gap from thermal excitation. The gap values obtained from the slopes of the pristine (pink dashed line) and the lightly substituted samples (green dashed line) above 20 K (dotted vertical line) are given.

further out compared to nonmagnetic impurities. In the former case, the formation of a global conducting surface state in SmB_6:3%Gd at low *T* is already inhibited, providing a microscopic picture of how the topologically protected surface state is destroyed in real space.

DISCUSSION

Now, the pressing question concerns the underlying mechanism for the suppression of the surface state signature peak in STS in both cases, for magnetic tips and magnetic substituents in SmB_6. The observed disappearance of the peaks at −6.5 and −2.5 meV upon tunneling with magnetic tips or on surfaces of Gd-substituted samples could be either due to suppression of the actual surface states or due to simply suppressing the tunneling probability into the corresponding states (or a combination thereof). Although we cannot unambiguously distinguish between these two scenarios, we consider the similarity of the spectra with suppressed surface state signature peak to those obtained on pristine SmB_6 with a W tip (*7*) at $T = 20$ K, i.e., a temperature at which the surface states are not visible in the tunneling spectra, as a strong indication toward the former, i.e., a repressed formation of the surface state (see fig. S4). The consistency with our theocratical model is also in line with this conclusion. In such a case, the main parameter determining the extent of the suppressed surface state around a magnetic impurity is related to the exchange interaction (*29*). Moreover, the surface state suppression via magnetic tips calls for an interaction whose energy scale is well beyond the Zeeman energy scale associated with a magnetic field of 12 T (Fig. 1). Therefore, we propose an exchange interaction–based proximity effect to be involved when tunneling with a magnetic tip or around a magnetic substituent.

Our findings have two important consequences. First, they provide a microscopic picture of how the surface states are perturbed by impurities. This pertubation takes place locally at the defect site, with an extent ℓ_{sup} that depends on the magnetic properties of the defect. Enhanced values of ℓ_{sup} and, particularly, h_{sup} at magnetic substituents as observed via our STM experiments were considered a hallmark for TSSs (*29*). Second, the very effective suppression of the surface state signature peak at −6.5 meV can be exploited in applications. We propose to use SmB_6 to detect exchange fields: If a tunneling tip is made of SmB_6 and scanned over a surface to be investigated, then the dI/dV response at $V_b = -6.5$ mV is expected to change substantially around a magnetic surface atom. On the basis of our investigations by magnetic tips and magnetic impurities, this effect should allow for single spin detection.

MATERIALS AND METHODS

Sample preparation

All samples used in this study were grown by the Al-flux method (*8*). Single crystals were aligned by Laue diffraction and mounted, such that the subsequent cleave exposes a {001} surface. Cleaving was conducted in situ below 20 K. Subsequent STM topography confirmed the sample orientation. For pristine SmB_6, six different single crystals were cleaved and investigated for this study, and for SmB_6:0.5%Gd and SmB_6:3%Y, three single crystals were investigated.

Pristine SmB_6 samples are difficult to cleave, and atomically flat and well-resolved surface areas have to be searched for. By introducing substituents into SmB_6, the cleavage properties change markedly, and atomically flat areas can be found much more easily. However, the vast majority of the surface areas investigated so far was reconstructed (see also text S3 and fig. S5). Again, unreconstructed surface areas have to be searched for.

Details of tunneling measurements

STM measurements were conducted in an ultrahigh vacuum ($p < 3 \times 10^{-9}$ Pa) environment and at a temperature $T = 0.35$ K. The tunneling current *I* was measured using tungsten tips or Cr-coated tips. Tunneling parameters for topography, if not noted otherwise, were $V_b = 300$ mV and $I_{sp} = 200$ pA. The dI/dV spectra were acquired by a lock-in technique applying a modulation voltage of typically $V_{mod} = 0.3$ mV; if enhanced resolution was strived for, V_{mod} was reduced to 0.05 mV. The bias voltage V_b is applied to the sample. A magnetic field of up to 12 T can be applied perpendicular to the scanned sample surface.

Scanning tunneling spectroscopy using Cr tips

For spin-polarized scanning tunneling spectroscopy, commercially available Cr-coated tips (NaugaNeedles LLC: http://nauganeedles.com/products-USSTM-W500-Cr) were used. These tips are characterized by uncompensated magnetic moments at the Cr tip apex, resulting in a spin polarization (up to 45%) at the Fermi level (*22*). In addition to STS on SmB_6 with magnetic tips in zero field, these measurements have also been conducted in magnetic fields. Selected results of one of the field cycles are shown in fig. S1. Here, the magnetic field (applied perpendicular to the sample surface) was gradually increased up to $\mu_0 H = 5$ T, consecutively ramped back down to zero field, and reversed, with spectra taken at constant field values. No significant change in the tunneling spectra was observed. The dI/dV data perfectly overlapped in the low-field regime; i.e., weak antilocalization effects were not

visible in our tunneling spectra. At high magnetic fields, the zero-bias conductance was slightly reduced. Such a high applied field may influence the magnetization orientation within our magnetic tip, which, in turn, can reduce the tunneling current through spin-polarized effects. Notably, scanning the Cr tip over substantial surface areas of pristine SmB_6 alludes toward the lack of any significant local dependencies of the spectra.

SUPPLEMENTARY MATERIALS

Supplementary material for this article is available at http://advances.sciencemag.org/cgi/content/full/4/11/eaau4886/DC1

Text S1. Changing tip conditions on Gd-substituted SmB_6
Text S2. Comparison of spectra with suppressed surface state signature peak
Text S3. Reconstructed surface of Gd-substituted SmB_6
Text S4. Comparison between SmB_6:0.5%Gd and SmB_6:3%Gd
Text S5. Defect analysis of SmB_6:3%Y
Text S6. Analytical solution to the single magnetic impurity
Fig. S1. STS with a Cr tip in a magnetic field.
Fig. S2. Converting a nonmagnetic into a magnetic tip.
Fig. S3. Topographies obtained with a W tip on SmB_6:0.5%Gd.
Fig. S4. Suppression of the surface state signature peak.
Fig. S5. Disordered reconstructed surface of SmB_6:0.5%Gd.
Fig. S6. Suppression of surface state signature peak on SmB_6:3%Gd.
Fig. S7. Surface of SmB_6:3%Y.

REFERENCES AND NOTES

1. L. Fu, C. L. Kane, Superconducting proximity effect and Majorana fermions at the surface of a topological insulator. *Phys. Rev. Lett.* **100**, 096407 (2008).
2. R. Zitko, Quantum impurity on the surface of a topological insulator. *Phys. Rev. B* **81**, 241414 (2010).
3. M. Dzero, K. Sun, V. Galitski, P. Coleman, Topological Kondo insulators. *Phys. Rev. Lett.* **104**, 106408 (2010).
4. T. Takimoto, SmB_6: A promising candidate for a topological insulator. *J. Phys. Soc. Jpn.* **80**, 123710 (2011).
5. F. Lu, J. Zhao, H. Weng, Z. Fang, X. Dai, Correlated topological insulators with mixed valence. *Phys. Rev. Lett.* **110**, 096401 (2013).
6. Y. S. Eo, A. Rakoski, J. Lucien, D. Mihaliov, C. Kurdak, P. Ferrari Silveira Rosa, D.-J. Kim, Z. Fisk, Robustness of the insulating bulk in the topological Kondo insulator SmB_6. arXiv:1803.00959 [cond-mat.str-el] (2 March 2018).
7. L. Jiao, S. Rößler, D. J. Kim, L. H. Tjeng, Z. Fisk, F. Steglich, S. Wirth, Additional energy scale in SmB_6 at low temperature. *Nat. Commun.* **7**, 13762 (2016).
8. D. J. Kim, J. Xia, Z. Fisk, Topological surface state in the Kondo insulator samarium hexaboride. *Nat. Mater.* **13**, 466–470 (2014).
9. G. Schubert, H. Fehske, L. Fritz, M. Vojta, Fate of topological-insulator surface states under strong disorder. *Phys. Rev. B* **85**, 201105 (2012).
10. S. Wolgast, C. Kurdak, K. Sun, J. W. Allen, D.-J. Kim, Z. Fisk, Low-temperature surface conduction in the Kondo insulator SmB_6. *Phys. Rev. B* **88**, 180405 (2013).
11. D. J. Kim, S. Thomas, T. Grant, J. Botimer, Z. Fisk, J. Xia, Surface Hall effect and nonlocal transport in SmB_6: Evidence for surface conduction. *Sci. Rep.* **3**, 3150 (2013).
12. H. Miyazaki, T. Hajiri, T. Ito, S. Kunii, S. I. Kimura, Momentum-dependent hybridization gap and dispersive in-gap state of the Kondo semiconductor SmB_6. *Phys. Rev. B* **86**, 075105 (2012).
13. Z.-H. Zhu, A. Nicolaou, G. Levy, N. P. Butch, P. Syers, X. F. Wang, J. Paglione, G. A. Sawatzky, I. S. Elfimov, A. Damascelli, Polarity-driven surface metallicity in SmB_6. *Phys. Rev. Lett.* **111**, 216402 (2013).
14. P. Hlawenka, K. Siemensmeyer, E. Weschke, A. Varykhalov, J. Sánchez-Barriga, N. Y. Shitsevalova, A. V. Dukhnenko, V. B. Filipov, S. Gabáni, K. Flachbart, O. Rader, E. D. L. Rienks, Samarium hexaboride is a trivial surface conductor. *Nat. Commun.* **9**, 517 (2018).
15. N. Xu, P. K. Biswas, J. H. Dil, R. S. Dhaka, G. Landolt, S. Muff, C. E. Matt, X. Shi, N. C. Plumb, M. Radović, E. Pomjakushina, K. Conder, A. Amato, S. V. Borisenko, R. Yu, H.-M. Weng, Z. Fang, X. Dai, J. Mesot, H. Ding, M. Shi, Direct observation of the spin texture in SmB_6 as evidence of the topological Kondo insulator. *Nat. Commun.* **5**, 4566 (2014).
16. S. Suga, K. Sakamoto, T. Okuda, K. Miyamoto, K. Kuroda, A. Sekiyama, J. Yamaguchi, H. Fujiwara, A. Irizawa, T. Ito, S. Kimura, T. Balashov, W. Wulfhekel, S. Yeo, F. Iga, S. Imada, Spin-polarized angle-resolved photoelectron spectroscopy of the so-predicted Kondo topological insulator SmB_6. *J. Phys. Soc. Jpn* **83**, 014705 (2014).
17. Q. Song, J. Mi, D. Zhao, T. Su, W. Yuan, W. Xing, Y. Chen, T. Wang, T. Wu, X. Hui Chen, X. C. Xie, C. Zhang, J. Shi, W. Han, Spin injection and inverse Edelstein effect in the surface states of topological Kondo insulator SmB_6. *Nat. Commun.* **7**, 13485 (2016).
18. S. Rößler, L. Jiao, D. J. Kim, S. Seiro, K. Rasim, F. Steglich, L. H. Tjeng, Z. Fisk, S. Wirth, Surface and electronic structure of SmB_6 through scanning tunneling microscopy. *Philos. Mag.* **96**, 3262–3273 (2016).
19. M. M. Yee, Y. He, A. Soumyanarayanan, D.-J. Kim, Z. Fisk, J. E. Hoffman, Imaging the Kondo insulating gap on SmB_6. arXiv:1308.1085 [cond-mat.str-el] (27 August 2013).
20. S. Rößler, T.-H. Jang, D.-J. Kim, L. H. Tjeng, Z. Fisk, F. Steglich, S. Wirth, Hybridization gap and Fano resonance in SmB_6. *Proc. Natl. Acad. Sci. U.S.A.* **111**, 4798–4802 (2014).
21. W. Ruan, C. Ye, M. Guo, F. Chen, X. Chen, G.-M. Zhang, Y. Wang, Emergence of a coherent in-gap state in the SmB_6 Kondo insulator revealed by scanning tunneling spectroscopy. *Phys. Rev. Lett.* **112**, 136401 (2014).
22. H. Oka, O. O. Brovko, M. Corbetta, V. S. Stepanyuk, D. Sander, J. Kirschner, Spin-polarized quantum confinement in nanostructures: Scanning tunneling microscopy. *Rev. Mod. Phys.* **86**, 1127 (2014).
23. A. Schlenhoff, S. Krause, G. Herzog, R. Wiesendanger, Bulk Cr tips with full spatial magnetic sensitivity for spin-polarized scanning tunneling microscopy. *Appl. Phys. Lett.* **97**, 083104 (2010).
24. M. Enayat, Z. Sun, U. Raj Singh, R. Aluru, S. Schmaus, A. Yaresko, Y. Liu, C. Lin, V. Tsurkan, A. Loidl, J. Deisenhofer, P. Wahl, Real-space imaging of the atomic-scale magnetic structure of $Fe_{1+y}Te$. *Science* **345**, 653–656 (2014).
25. P. P. Baruselli, M. Vojta, Spin textures on general surfaces of the correlated topological insulator SmB_6. *Phys. Rev. B* **93**, 195117 (2016).
26. M. Corbetta, S. Ouazi, J. Borme, Y. Nahas, F. Donati, H. Oka, S. Wedekind, D. Sander, J. Kirschner, Magnetic response and spin polarization of bulk Cr tips for in-field spin-polarized scanning tunneling microscopy. *Jpn. J. Appl. Phys.* **51**, 030208 (2012).
27. Z. Sun, A. Maldonado, W. S. Paz, D. S. Inosov, A. P. Schnyder, J. J. Palacios, N. Y. Shitsevalova, V. B. Filipov, P. Wahl, Observation of a well-defined hybridization gap and in-gap states on the SmB_6 (001) surface. *Phys. Rev. B* **97**, 235107 (2018).
28. Y. Luo, H. Chen, J. Dai, Z. Xu, J. D. Thompson, Heavy surface state in a possible topological Kondo insulator: Magnetothermoelectric transport on the (011) plane of SmB_6. *Phys. Rev. B* **91**, 075130 (2015).
29. Q. Liu, C.-X. Liu, C. Xu, X.-L. Qi, S.-C. Zhang, Magnetic impurities on the surface of a topological insulator. *Phys. Rev. Lett.* **102**, 156603 (2009).
30. Q.-H. Wang, D. Wang, F.-C. Zhang, Electronic structure near an impurity and terrace on the surface of a three-dimensional topological insulator. *Phys. Rev. B* **81**, 035104 (2010).
31. R. R. Biswas, A. V. Balatsky, Impurity-induced states on the surface of three-dimensional topological insulators. *Phys. Rev. B* **81**, 233405 (2010).
32. J. Figgins, D. K. Morr, Defects in heavy-Fermion materials: Unveiling strong correlations in real space. *Phys. Rev. Lett.* **107**, 066401 (2011).
33. W. T. Fuhrman, J. R. Chamorro, P. A. Alekseev, J.-M. Mignot, T. Keller, J. A. Rodriguez-Rivera, Y. Qiu, P. Nikolić, T. M. McQueen, C. L. Broholm, Screened moments and extrinsic in-gap states in samarium hexaboride. *Nat. Commun.* **9**, 1539 (2018).
34. F. Yang, Y. R. Song, H. Li, K. F. Zhang, X. Yao, C. Liu, D. Qian, C. L. Gao, J.-F. Jia, Identifying magnetic anisotropy of the topological surface state of $Cr_{0.02}Sb_{1.95}Te_3$ with spin-polarized STM. *Phys. Rev. Lett.* **111**, 176802 (2013).
35. Y. Jiang, C. Song, Z. Li, M. Chen, R. L. Greene, K. He, L. Wang, X. Chen, X. Ma, Q.-K. Xue, Mass acquisition of Dirac fermions in magnetically doped topological insulator Sb_2Te_3 films. *Phys. Rev. B* **92**, 195418 (2015).
36. I. Lee, C. Koo Kim, J. Lee, S. J. L. Billinge, R. Zhong, J. A. Schneeloch, T. Liu, T. Valla, J. M. Tranquada, G. Gu, J. C. Séamus Davis, Imaging Dirac-mass disorder from magnetic dopant atoms in the ferromagnetic topological insulator $Cr_x(Bi_{0.1}Sb_{0.9})_{2-x}Te_3$. *Proc. Natl. Acad. Sci. U.S.A.* **112**, 1316 (2015).
37. P. Sessi, R. R. Biswas, T. Bathon, O. Storz, S. Wilfert, A. Barla, K. A. Kokh, O. E. Tereshchenko, K. Fauth, M. Bode, A. V. Balatsky, Dual nature of magnetic dopands and competing trends in topological insulators. *Nat. Commun.* **7**, 12027 (2016).
38. T. Valla, Z.-H. Pan, D. Gardner, Y. S. Lee, S. Chu, Photoemission spectroscopy of magnetic and nonmagnetic impurities on the surface of the Bi_2Se_3 topological insulator. *Phys. Rev. Lett.* **108**, 117601 (2012).
39. K. Flachbart, K. Gloos, E. Konovalova, Y. Paderno, M. Reiffers, P. Samuely, P. Švec, Energy gap of intermediate-valent SmB_6 studied by point-contact spectroscopy. *Phys. Rev. B* **64**, 085104 (2001).
40. M. Orendá, S. Gabáni, G. Pristáš, E. Gažo, P. Diko, P. Farkašovský, A. Levchenko, N. Shitsevalova, K. Flachbart, Isosbestic points in doped SmB_6 as features of universality and property tuning. *Phys. Rev. B* **96**, 115101 (2017).

Acknowledgments: We acknowledge valuable discussion with P.-Y. Chang, P. Coleman, O. Erten, M. H. Hamidian, D. J. Kim, M. Nicklas, D. Sander, L. H. Tjeng, and B. Yan. **Funding:** This work was supported by the DFG through SPP 1666. L.J. acknowledges support from the Alexander von Humboldt Foundation. P.F.S.R. acknowledges support from the Laboratory

Directed Research and Development Program of Los Alamos National Laboratory under project number 20160085DR. H.Y. acknowledges support from the National Key R&D Program of China (grant nos. 2017YFA0303100 and 2016YFA0300202), the National Natural Science Foundation of China (grant no. U1632275), and the Science Challenge Project of China (project no. TZ2016004). C.-X.L. acknowledges support through ONR grant N00014-15-1-2675. Z.F. acknowledges support from NSF through DMR1708199. **Author contributions:** S.W., Z.F., and F.S. designed the research. L.J. and S.R. conducted the STM experiments. L.J., S.R., C.G., and H.Y. performed electronic transport measurements. P.F.S.R. and Z.F. provided the samples. D.K. and C.-X.L. provided theoretical insight. All authors contributed to the discussions and the manuscript. **Competing interests:** The authors declare that they have no competing interests. **Data and materials availability:** All data needed to evaluate the conclusions in the paper are present in the paper and/or the Supplementary Materials. Additional data related to this paper may be requested from the corresponding authors.

Submitted 15 June 2018
Accepted 12 October 2018
Published 9 November 2018
10.1126/sciadv.aau4886

Citation: L. Jiao, S. Rößler, D. Kasinathan, P. F. S. Rosa, C. Guo, H. Yuan, C.-X. Liu, Z. Fisk, F. Steglich, S. Wirth, Magnetic and defect probes of the SmB_6 surface state. *Sci. Adv.* **4**, eaau4886 (2018).